Clim Dyn (2016) 47:3191–3202
DOI 10.1007/s00382-016-3020-z

Multi-year wind dynamics around Lake Tanganyika

D. Docquier[1] · W. Thiery[1] · S. Lhermitte[1] · N. van Lipzig[1]

Received: 7 September 2015 / Accepted: 3 February 2016 / Published online: 12 February 2016

Abstract Lake Tanganyika is the second largest freshwater lake in the world by volume and is of prime importance for the regional economy in East Africa. Although the lake is recognized as a key component of the regional climate system, little is known about atmospheric dynamics in its surroundings. To understand this role, we analyze winds around Lake Tanganyika as modeled by a high resolution (7 km) regional climate model (Consortium for Small-scale Modeling in Climate Mode) over the period 1999–2008. Modeled surface wind speed and direction are in very good agreement with high resolution (12.5 km) Quick Scatterometer (QuikSCAT) satellite wind observations during the dry season. Comparison of a control run with a model simulation where all lake pixels are replaced by representative land pixels indicates that mean surface wind speed over Lake Tanganyika almost doubles due to lake presence. Furthermore, a region of higher surface wind speed in the central part of the lake is identified and confirmed by QuikSCAT observations. A combination of wind channeling along valley mountains and wind confluence on the upwind side of the lake is responsible for this speed-up. The lower wind speeds in the rest of the lake result from blocked conditions due to more pronounced orography. Finally, the model captures a zone of higher wind speed at around 2 km height, associated with the low-level Somali jet. These results demonstrate that high resolution climate modeling allows a detailed understanding of wind dynamics in the vicinity of Lake Tanganyika.

✉ D. Docquier
docquier.david@gmail.com

[1] Department of Earth and Environmental Sciences, K.U.Leuven, Celestijnenlaan 200E, 3001 Louvain, Belgium

Keywords Lake Tanganyika · Wind · Regional climate model · Orography

1 Introduction

Lake Tanganyika is located in the East African Great Rift Valley between Democratic Republic of Congo in the west, Burundi in the northeast, Tanzania in the east and Zambia in the south. The lake is relatively long (∼650 km) and narrow (∼50 km). It is the second largest freshwater lake in the world in terms of volume (18,900 km^3) and the second deepest (maximum depth of 1470 m). It is confined by valley mountains reaching up to 3000 m in the north and 2000 m in the south, while the central part around 6.5°S latitude is relatively flat (Fig. 1). The lake surface is at 773 m altitude.

Lake Tanganyika is of prime importance for both the regional economy and the regional climate. On the one hand, local population strongly depends on fish industry, drinking water and electricity production provided by the lake. On the other hand, the lake intensively interacts with the surrounding atmosphere in a complex way. The latter aspect is studied here.

Atmospheric circulation in East Africa is governed by (south)westerly Congo Air, and northeasterly and southeasterly monsoons (Nicholson 1996). Congo Air is thermally unstable and associated with rainfall, while both monsoons are thermally stable and relatively dry.

The region around Lake Tanganyika experiences a cool (∼25 °C) dry season from May to September and a warm (∼28 °C) wet season from October to April (Verburg and Hecky 2003). Savijärvi and Järvenoja (2000) identify a long rain season in March–April, a main dry season from June to August and a short rain season in October–November. The

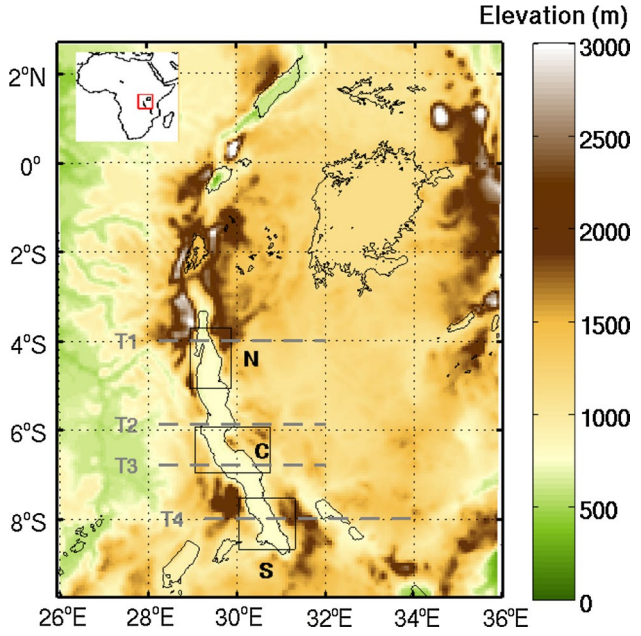

Fig. 1 Surface elevation of the model domain [*source*: Global Land One-kilometer Base Elevation (GLOBE), Hastings et al. (1999)]. *Rectangles* denote the three lake regions, each including 135 model pixels (*N*, *C* and *S* stand for north, center and south respectively). *Dashed gray lines* show the four transects analyzed in this study (*T1*, *T2*, *T3*, *T4*)

dry season is characterized by relatively strong southeasterly winds, while weaker winds blow during the wet season (Savijärvi 1997; Verburg and Hecky 2003).

Winds around Lake Tanganyika are influenced by the Intertropical Convergence Zone (ITCZ) dynamics (trade winds), orography (slope winds) and lake thermal effect (lake and land breezes). According to a two-dimensional mesoscale model integration during three consecutive days in July, half of the diurnal wind variation is caused by slope winds, one quarter is due to lake and land breezes, and the last quarter comes from trade winds (Savijärvi 1997). In addition, the High Resolution Limited Area Model (HIRLAM) is integrated at a resolution of 5.5 km over the Lake Tanganyika region during the months of March and July 1994 and allows to identify high lake evaporation in July (dry season) and land evaporation in March (wet season) (Savijärvi and Järvenoja 2000).

Wind patterns observed at three automatic weather land stations and two offshore buoys around the lake over the period 1993–1996 show (daytime) lake and (nighttime) land breezes enhanced by southeasterly trade winds (Verburg and Hecky 2003). The atmosphere above Lake Tanganyika is almost always unstable due to higher lake surface water temperature (LSWT) compared to the overlying surface air (Verburg and Antenucci 2010). This instability leads to an increase in heat loss by latent and sensible heat fluxes.

The impact of African Great Lakes on atmospheric dynamics and hydrological cycle is assessed in Thiery et al. (2015). In the latter study, the Consortium for Small-scale Modeling in Climate Mode (COSMO-CLM, version 4.8) coupled to both the Community Land Model (CLM version 3.5) and the one-dimensional Freshwater Lake model (FLake) is used to dynamically downscale a Coordinated Regional Climate Downscaling Experiment for Africa (CORDEX-Africa) at a 7-km horizontal resolution over the period 1999–2008. The model is extensively evaluated in terms of LSWT, precipitation, air temperature and surface energy fluxes against different dataset. A good model performance is found for the first two parameters with a slightly warm LSWT model bias. Furthermore, the African Great Lakes have a cooling effect on the surrounding atmosphere (−0.6 to −0.9 °C on average) and almost double annual precipitation over their surface. This study clearly shows the added value of resolving individual lakes with a high resolution climate model (Thiery et al. 2015).

During the last century (1913–2000), the lake water temperature has increased by ∼1.3 °C at the surface and ∼0.2 °C at 1000 m depth (Verburg and Hecky 2009; Kraemer et al. 2015). This differential heating over depth is responsible for a reduction in biological productivity due to reduced vertical mixing. The recent increase in LSWT and decrease in primary productivity exceed the natural variability range (Tierney et al. 2010). The projected warming in East Africa [0.5–6 °C by the end of the century relative to present-day climate; Niang et al. (2014)] could exacerbate the risks for natural species living in the lake, and thus local economies depending on the lake. Moreover, the growing human population in the region will contribute to the ongoing deforestation, which could induce an additional warming of about 0.7 °C by 2050 (Akkermans et al. 2013, 2014).

In the current global warming context, the economic role of Lake Tanganyika in feeding local population is threatened and the whole region could experience severe weather changes. It is thus highly important to understand the regional climate that surrounds Lake Tanganyika. The present paper aims at providing more accurate details about one of the key elements of the regional climate, namely wind, in the region surrounding Lake Tanganyika using COSMO-CLM model coupled to both land and lake models. This is the first time that a high-resolution regional climate model including a lake model is used on such a long period (from 1999 to 2008) to analyze wind climatology in the region around Lake Tanganyika. This is also the first time that wind model outputs for Lake Tanganyika are compared to satellite data (Quick Scatterometer [QuikSCAT]). Seasonal, intraseasonal and diurnal variabilities of wind speed are investigated in order to provide a temporal analysis. Furthermore, the lake effect on wind is investigated by comparing the control run to a simulation without

lakes (where all lake pixels are replaced by representative land pixels). Finally, Lake Tanganyika is located in a valley surrounded by high mountains, so the impact of orography on wind speed and direction plays a key role and is analyzed in this study.

2 Methodology

The three-dimensional non-hydrostatic COSMO-CLM model (version 4.8) is used to simulate present-day climate (1999–2008) in East Africa. COSMO-CLM is coupled to the Community Land Model [CLM version 3.5, Davin and Seneviratne (2012)] instead of the default TERRA-ML scheme, due the strong improvement in the representation of the partitioning of the turbulent fluxes and consequently the near-surface meteorological conditions on the African continent (Akkermans et al. 2012). In addition, COSMO-CLM is coupled to the one-dimensional lake model FLake (Mironov et al. 2010; Thiery et al. 2014a, b), which shows good performance over the East African Great Lakes (Thiery et al. 2015). The coupled model, hereafter referred to as COSMO-CLM^2, uses the COSMO-CLM CORDEX-Africa data as lateral boundary conditions, which is in turn driven by ERA-Interim.

Two experiments are performed at a horizontal resolution of 0.0625° (∼7 km) using 50 vertical levels and a time step of 60 s, namely 'control' (CTL) and 'no lake' (NOL) simulations. The model domain ranges from ∼2°N to 10°S latitude and ∼26°E to 36°E longitude and therewith encompasses most of the African Great Lakes (Fig. 1). Lake Tanganyika is represented by 683 model pixels at that resolution. The only difference between CTL and NOL experiments is that lake pixels are replaced by representative land pixels in NOL. Representative land pixels are randomly selected from all land pixels within a distance of 50 km. Since not all lake pixels have land pixels within 50 km distance, this procedure is repeated until all lake pixels are eventually replaced. When not mentioned in the following text and figures, the CTL simulation is used. A more detailed description of the model and both experiments can be found in Thiery et al. (2015).

The second simulation (hereafter referred to as NOL) is identical to the control experiment, except that each lake pixel is replaced by a representative land pixel selected from all land pixels within a distance of 50 km. The representative land pixel was chosen through random selection from a all land pixels within this radius. Since not all lake pixels had land within 50 km distance, this procedure was repeated until all lake pixels were eventually replaced.

In this study, we evaluate modeled wind speed against wind speed provided by QuikSCAT at a horizontal resolution of 12.5 km using the QuikSCAT L2B product (Fore et al. 2014). QuikSCAT carries the Sea Winds scatterometer that allows for wind speed and direction measurements over oceans and lakes from June 1999 to November 2009 (Nghiem et al. 2004; Bentamy et al. 2012). Data are provided twice a day (06:00 and 18:00 local solar time). QuikSCAT data are retrieved for all pixels with available data. Data with a usable rain flag are included in the analysis since they are corrected for rain contamination (Fore et al. 2014).

In order to better account for the spatial wind distribution, Lake Tanganyika is divided into three different lake regions (north, center and south). The north and south regions are surrounded by high mountains, while a relatively smoother terrain is present around the lake center. In each region, a fixed amount of 135 pixels (∼6500 km^2) is taken (Fig. 1).

Four transects crossing Lake Tanganyika in an east-west direction are chosen to analyze vertical wind profiles at different places: one in the north (T1 at 4°S), two in the center (T2 at 5.9°S, and T3 at 6.8°S) and one in the south (T4 at 8°S) (Fig. 1). Along these four transects, the internal Froude number Fr is identified to characterize the ability of the air to flow over the mountains surrounding the lake. Fr is calculated on the dominant upwind side of the mountain range as follows (Wallace and Hobbs 2006; van Lipzig et al. 2008):

$$Fr = \frac{u}{N \times h}, \tag{1}$$

where u is the zonal wind speed (east-west direction), h the mountain height and N the Brunt-Väisälä frequency, which is derived from Reinecke and Durran (2008):

$$N = \sqrt{\frac{g}{\theta}\frac{\partial\theta}{\partial z}}, \tag{2}$$

with g being the gravitational acceleration (set to 9.81 m s^{-2}), θ the potential air temperature, and z the surface elevation. u and N are vertically averaged between mountain bottom and top and calculated at least one mountain height range away from the mountain bottom (see Fig. 11 for the location of u and N calculations). Note that N (and thus Fr) can only be computed when $\partial\theta/\partial z > 0$. θ is computed following Holton (2004, eq. (2.44)):

$$\theta = T\left(\frac{p_s}{p}\right)^{\frac{R}{c_p}}, \tag{3}$$

where T is the air temperature, p_s the standard reference atmospheric pressure (set to 101 325 Pa), p the atmospheric pressure, R the gas constant for dry air (set to 287 J kg^{-1} K^{-1}) and c_p the specific heat capacity of dry air at constant pressure (set to 1004 J kg^{-1} K^{-1}). Low Fr values ($Fr < 1$) mean that low-level air flow is forced to go around the mountain (blocked conditions), while high

values ($Fr > 1$) mean that the flow goes over the mountain (flow-over conditions).

To assess the persistence of wind regimes at a particular location, we compute the directional constancy DC, which is the ratio of mean vector wind speed $\left|\overrightarrow{V}\right|$ over mean scalar wind speed $\overline{WS}$:

$$DC = \frac{\left|\overrightarrow{V}\right|}{\overline{WS}} = \frac{\sqrt{\overline{u}^2 + \overline{v}^2}}{\overline{WS}} = \frac{\sqrt{\left(\frac{1}{n}\sum_{i=1}^{n} u_i\right)^2 + \left(\frac{1}{n}\sum_{i=1}^{n} v_i\right)^2}}{\frac{1}{n}\sum_{i=1}^{n} WS_i}, \tag{4}$$

where v is the meridional wind speed (north-south direction), WS the scalar wind speed and n the number of observations in time. A value of $DC = 1$ means that wind direction does not change over the time period, indicating that the flow is largely controled by local topography. A value of DC close to 0 means that wind direction is highly random over time, i.e. wind blows equally frequently from all directions with the same mean speed.

Intraseasonal variability of daily wind speed is analyzed using the Fast Fourier Transform (FFT) in order to detect the presence of specific cycles within the seasons. The power spectrum PS of each year provides the strength of the signal at each frequency:

$$PS = \left|\sum_{k=0}^{n-1} c_k e^{-\frac{2\pi i}{n} jk}\right|^2 \qquad j = 0, \ldots, n-1 \tag{5}$$

where c_k is the value of the signal at time k, n is the number of time samples, j is the frequency. The mean interannual power spectrum is computed from the power spectra of all individual years.

3 Results

3.1 Model evaluation

A very good match between COSMO-CLM^2 and QuikSCAT is obtained from April to September in the morning (<0.2 m s^{-1} wind speed difference), which roughly corresponds to the dry season (Fig. 2). Wind speed differences are slightly higher in the evening but stay below 1 m s^{-1} from April to August and are equal to 1.4 m s^{-1} in September. In the wet season (October–March), observed wind speed is up to twice the modeled wind speed, which likely results from two effects. On the one hand, although QuikSCAT is corrected for rain effects, it is possible that remaining rain contamination still results in overestimation of wind speed in rainy conditions at low wind speeds (Fore et al. 2014), which typically occurs in the wet season. On the other hand, the model probably underestimates wind speed in the wet season, which may also explain the overestimated LSWT at that time (1–2 °C according to Thiery et al. (2015)).

Due to these constraints, we carry out the analysis with an emphasis on the dry season, and especially from May to August where model and observations agree quite well in the morning and evening. During this period, mean wind speed over Lake Tanganyika is 7 m s^{-1} in the morning and 4–5 m s^{-1} in the evening. Both model and observations

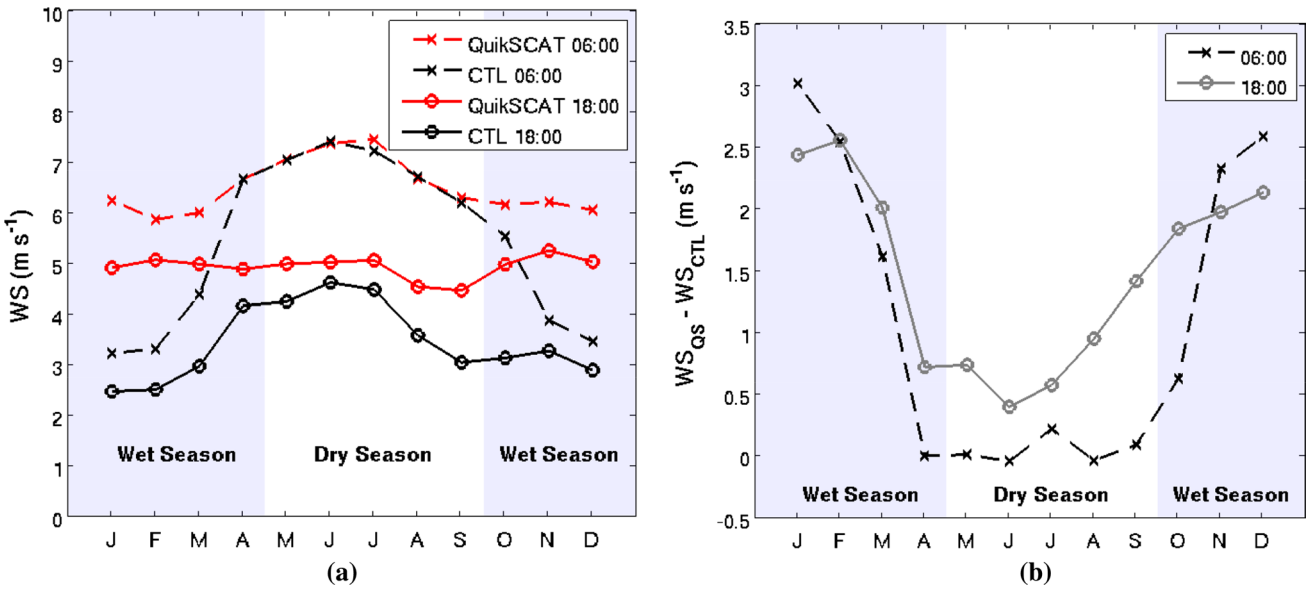

Fig. 2 **a** Monthly mean surface wind speed for the observations (QuikSCAT, 1999–2009) and the model (COSMO-CLM^2, 1999–2008) at 06:00 and 18:00. **b** Difference in monthly mean surface wind speed between observations and model at 06:00 and 18:00

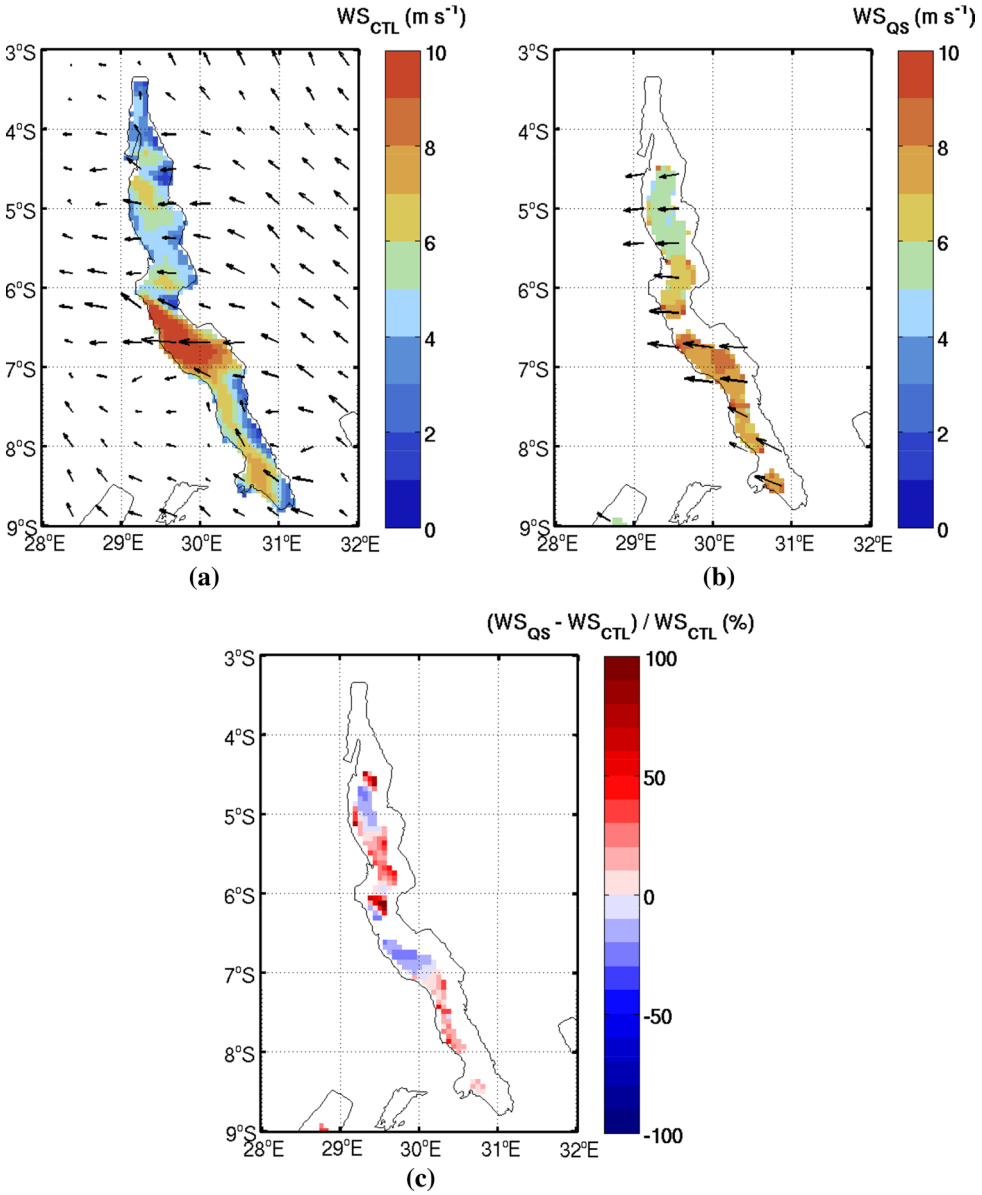

Fig. 3 Mean dry season (May–August) surface wind speed for **a** the model (COSMO-CLM^2, 1999–2008) and **b** observations (QuikSCAT, 1999–2009) at 06:00. Mean wind vectors are shown on both maps. **c** Relative difference between (**a**) and (**b**) with QuikSCAT data bilinearly interpolated onto the model grid

capture higher wind speed in the center and lower wind speed in the north compared to other lake regions (Fig. 3). The relative difference in wind speed between QuikSCAT and COSMO-CLM^2 is ∼60 % over the whole lake with some spatial variations (Fig. 3c). The mean wind direction is remarkably similar when comparing model (Fig. 3a) and observations (Fig. 3b), with a main easterly component (southeasterly in the south of the lake).

3.2 Seasonal, intraseasonal and diurnal winds

Over the entire period (1999–2008), highest modeled wind speeds over the lake are located in the center, ∼6.5°S latitude (Fig. 4). In terms of wind direction, southeasterly and easterly winds blow on the upwind (east) and downwind (west) sides of the lake. Over the lake, southerly winds are dominant in the north and south, and easterly winds blow in the center (Fig. 4).

When considering the seasonal cycle, mean wind speed is clearly higher during the dry season, with a peak in June, and lower during the wet season (Fig. 5). In terms of spatial variability, wind speed is highest in the lake center (5–7m s^{-1} during the dry season) and lowest in the north (2–3m s^{-1} during the wet season). Wind speed in the south is very close to mean wind speed over the whole lake.

Intraseasonal variability of the wind speed reveals large day-to-day changes with a clear transition from high wind speeds in the dry season (May–September, days 120–270 approximately) to low wind speeds in the wet season (rest of the year) (Fig. 6a). Interestingly, the FFT computed on

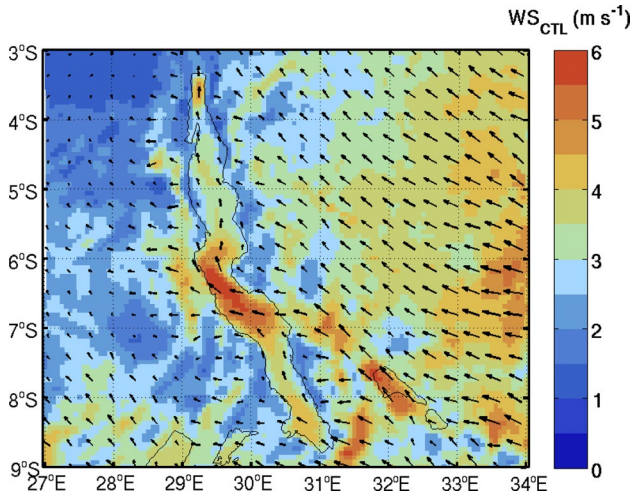

Fig. 4 Mean 10 m wind speed and direction simulated by COSMO-CLM^2 over 1999–2008

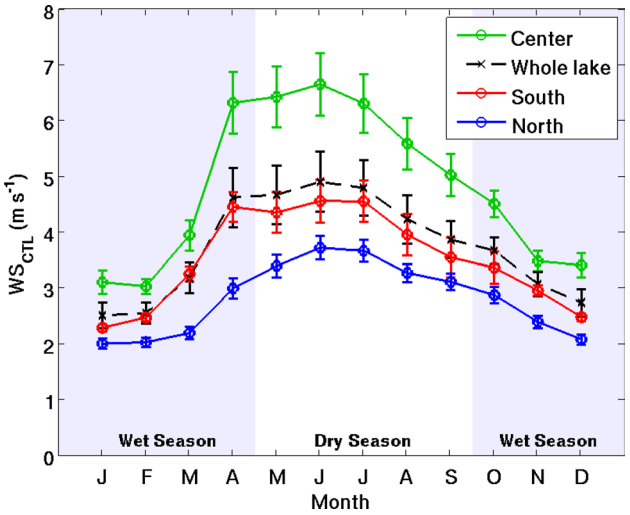

Fig. 5 Monthly mean 10 m wind speed simulated by COSMO-CLM^2 over 1999–2008 for the whole lake and three different regions. Standard deviation *bars* show the spatial variability within each region

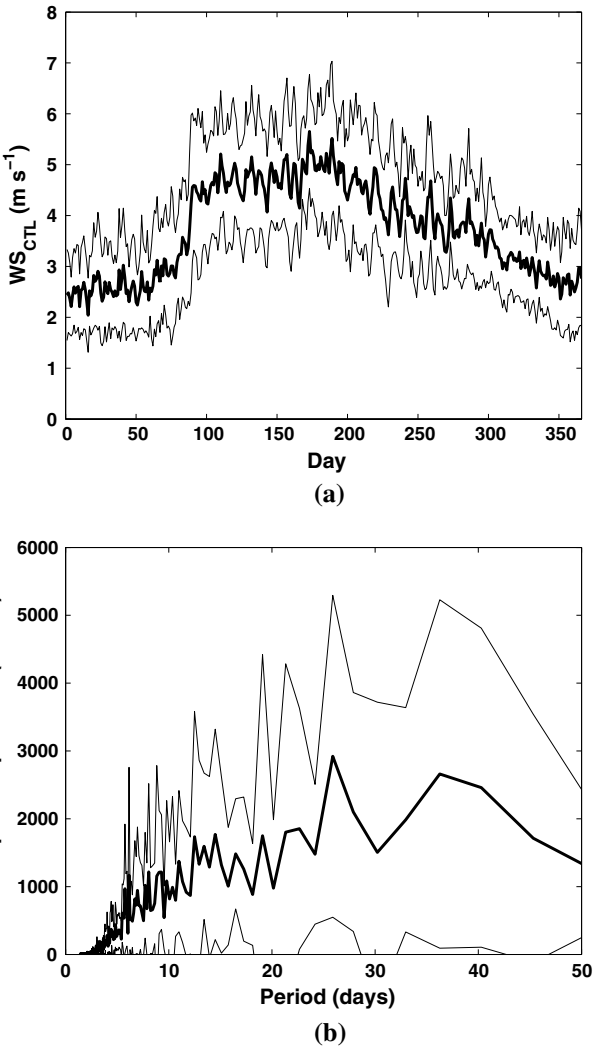

Fig. 6 **a** Daily mean interannual wind speed averaged over the period 1999–2008 and simulated by COSMO-CLM^2 (*thick line*) and interannual standard deviation around the mean (*thin lines*). **b** Mean interannual power spectrum of daily wind speed for each period (*thick line*) and interannual standard deviation around the mean (*thin lines*) based on the FFT computation over individual years from 1999 to 2008

daily wind speed allows to identify different cycles over the period 1999–2008. The dominant period in the mean interannual power spectrum is 26 days with secondary periods around 12, 21 and 36 days (Fig. 6b).

On a diurnal basis, modeled wind speed is highest in the early morning (03:00–06:00) for the whole lake average and center, at night (21:00–00:00) for the south and during the day (12:00) for the north (Fig. 7). In terms of spatial variability, the highest and lowest wind speeds are found in the center and north of the lake respectively. However, the south region has lower wind speed than the north around 12:00. High wind speed values in the north of the lake around 12:00 can be explained by the combination of lake breeze (wind from lake to land) and trade winds, which both come from the south/southeast at that time of the day and for that region. High wind speed values in the south around 00:00 are due to land breeze (wind from land to lake) and trade winds. The diurnal cycle is amplified during the dry season (Fig. 7a) compared to the wet season (Fig. 7b).

3.3 Lake effect

By comparing model simulations with (CTL) and without lakes (NOL), Lake Tanganyika enhances wind speed by $\sim$2 m s^{-1} ($\sim$80 %) during the dry season (Fig. 8). This

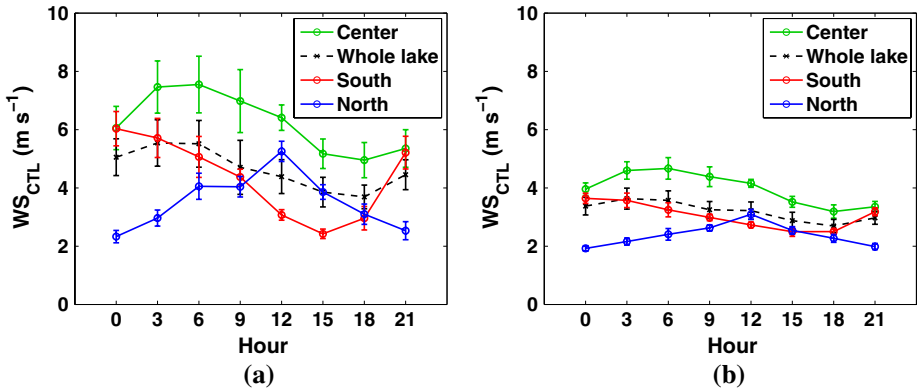

Fig. 7 Three-hourly mean 10 m wind speed simulated by COSMO-CLM^2 over **a** the dry season (May–August) and **b** wet season (October–April) of 1999–2008 for the whole lake and three different regions. Standard deviation *bars* show the spatial variability within each region

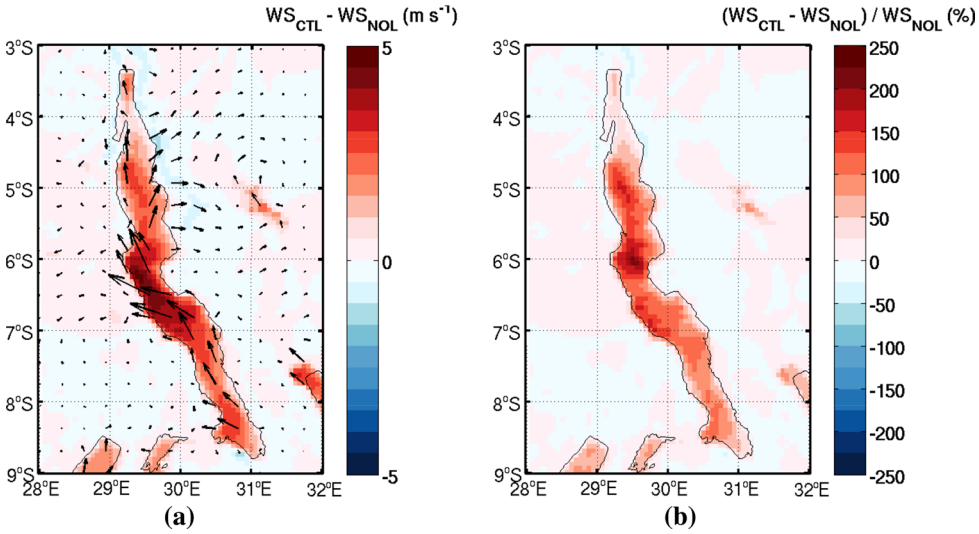

Fig. 8 **a** Difference in mean 10 m wind speed and direction between CTL and NOL simulations (May–August, 1999–2008). **b** Relative difference in mean 10 m wind speed between CTL and NOL simulations (May–August, 1999–2008)

feature is valid for all lakes of the model domain, including Lake Victoria and Lake Kivu (not shown). This mainly arises from lower surface roughness over lakes compared to roughness over land.

Wind speed difference between CTL and NOL simulations is highest in the center (up to 5 m s^{-1}; Fig. 8a). However, spatial variability is small in terms of relative difference (Fig. 8b). Lake-induced changes in wind direction are limited in the central and southern parts of the lake, while wind veering (clockwise from NOL to CTL) is modeled in the north (Fig. 8a).

The difference and relative difference between CTL and NOL wind speeds are highest in the early morning (03:00–06:00) (not shown). Thus, the lake plays a more important role in enhancing wind speed at that time of the day compared to any other time. However, the spatial variability in terms of relative difference between the two simulations remains small, suggesting a limited effect of the lake itself on wind speed spatial variability.

3.4 Impact of orography

High mountains are located around Lake Tanganyika in the north and south, and smaller mountains are present in the center (Fig. 9). Wind direction is affected by this variable orography: southeasterly winds blow on the upwind side of the central part of the lake and become easterly winds when flowing over the lake center (Fig. 9). In the north and south of the lake, southerly/southeasterly winds blow along the main lake axis due to channeling along rift valley mountains. This is especially obvious in the north, where mountains reach up to 3000 m (Fig. 9).

Wind speed is also influenced by orography. For instance, it is clearly lower in mountainous regions north and south of the lake (Figs. 4, 5, 7). Moreover, wind speed-up occurs in the lake center, which is confirmed by QuikSCAT observations (Fig. 3). This is probably due to both wind channeling along valley mountains and confluence of southeasterly and easterly flows on the upwind side of

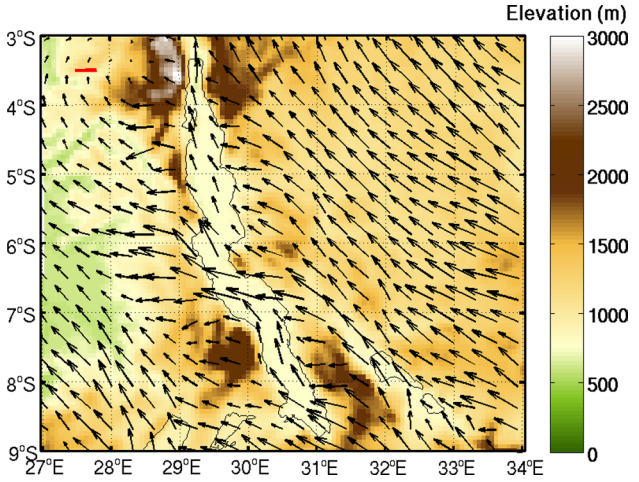

Fig. 9 Mean 10 m wind vectors simulated by COSMO-CLM^2 during the dry season (May–August) over 1999–2008 superimposed on elevation map. The *red line* in the *top left corner* of the *image* shows the scale of a wind speed equal to 3 m s^{-1}

the lake. On the one hand, topographic troughs are present at ∼6.8°S latitude on the eastern shore and ∼5.9°S on the western shore, leading to wind incursions over the lake from the eastern shore trough to the western shore trough and speed-up due to the narrow straight. Higher directional constancy (*DC*) values in the lake center compared to other lake regions confirm this channeling effect (Fig. 10). On the other hand, confluence of southeasterly and easterly flows on the upwind side of the eastern shore trough lead to further speed-up in the lake center.

A vertical cross-section analysis along the north (T1) and south (T4) transects shows the blocking effect ($Fr < 1$) of large-scale wind flow by mountains on the eastern shore (Figs. 11, 12). On the contrary, flow-over conditions ($Fr > 1$) are modeled in the center (T2 and T3) due to smoother terrain (Figs. 11, 12). Note that *Fr* can not be calculated between 09:00 and 15:00 due to decreasing potential air temperature θ with height during that timeframe, leading to complex values of Brunt-Väisälä frequency *N*.

Mean wind speed is highest at night (21:00–06:00) for all four transects, especially in the zone around 2 km height and for the central T2 and T3 transects (Fig. 11). The 2-km height zone is associated with the low-level Somali jet (Chakraborty et al. 2009). The presence of African orography, e.g. Great Rift Valley, greatly affects this low-level jet by enhancing the cross-equatorial flow (Chakraborty et al. 2009).

The difference in wind speed between CTL and NOL simulations also allows to identify lake and land breezes (not shown), as previously demonstrated by Thiery et al. (2015) in the case of Lake Victoria. During the day, a lake breeze occurs due to lower LSWT compared to land surface temperature, especially in the center (T2 and T3) where the orography is less pronounced. The lake breeze is weaker in the north (T1) and south (T4) due to the presence of higher mountains. A weak land breeze occurs at night.

4 Discussion

The highest wind speeds over the lake center confirm previous results with a high resolution (5.5 km) mesoscale model (Savijärvi and Järvenoja 2000). However, the latter study only considers the months of March and July 1994 and assumes that they are typical for wet and dry season respectively. Therefore, it does not capture the seasonal cycle and interannual variability. Furthermore, Savijärvi and Järvenoja (2000) perform a model validation limited to four weather stations around the lake. Finally, their model is not coupled to a lake model. Instead, LSWT is nudged towards the Lake Tanganyika Research (LTR) observations during the first day, and then kept fixed.

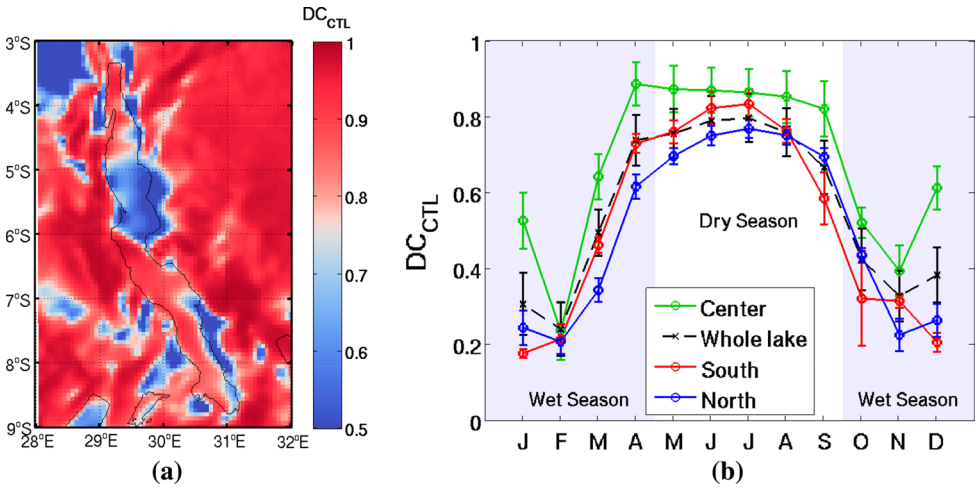

Fig. 10 **a** Directional constancy *DC* simulated by COSMO-CLM^2 for the dry season (May–August) over the period 1999–2008. **b** Monthly directional constancy over 1999–2008 for the whole lake and three different regions. Standard deviation *bars* are also shown

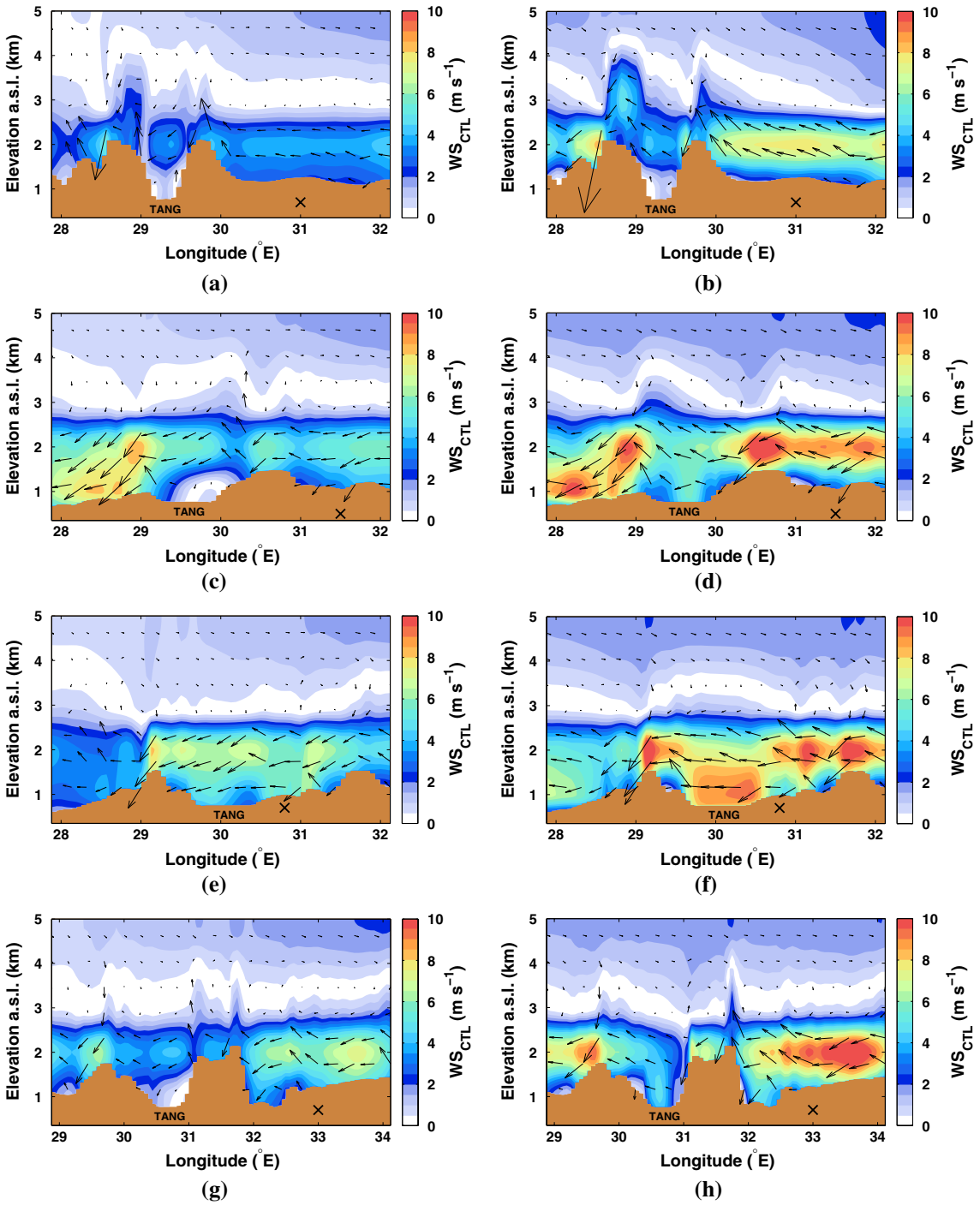

Fig. 11 *Vertical cross* sections of wind speed and direction simulated by COSMO-CLM^2 along four different transects over the 1999–2008 period (June to August) during day time (09:00–18:00; *left panels*) and night time (21:00–06:00; *right panels*). Lake Tanganyika is denoted by *TANG* and the *cross* indicates the longitude where internal Froude number is calculated for each transect. **a** T1 (4°S)—day (9:00–18:00), **b** T1 (4°S)—night (21:00–6:00), **c** T2 (5.9°S)—day (9:00–18:00), **d** T2 (5.9°S)—night (21:00–6:00), **e** T3 (6.8°S)—day (9:00–18:00), **f** T3 (6.8°S)—night (21:00–6:00), **g** T4 (8°S)—day (9:00–18:00), **h** T4 (8°S)—night (21:00–6:00)

Modeling results show that lake and land breezes are enhanced by southeasterly trade winds when they come from the same direction: winds in the north of the lake are stronger during the day due to lake breeze and trade winds flowing in the same direction, while winds in the south are stronger at night with land breeze and trade winds in the same direction (Fig. 7). This is in agreement with observational data coming from automatic sampling

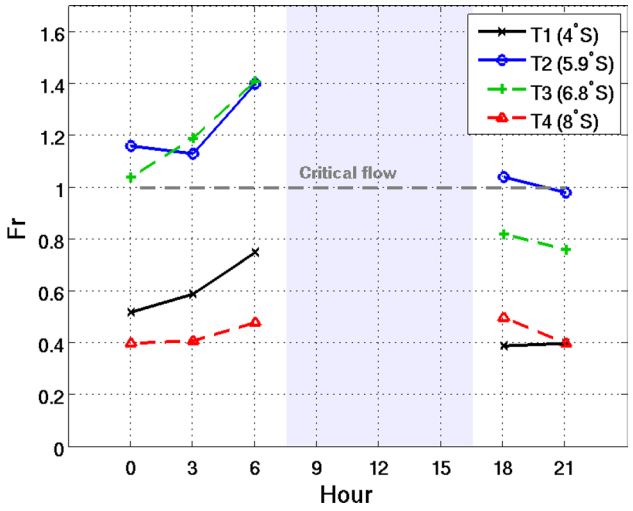

Fig. 12 Three-hourly mean internal Froude number *Fr* calculated using COSMO-CLM^2 output over the dry season (June–August) of 1999–2008 for the four transects. $Fr < 1$ means that air flow is forced to go around the mountain (blocked conditions), while $Fr > 1$ means that the flow goes over the mountain (flow-over conditions). *Fr* can not be calculated between 09:00 and 15:00 (*light blue area*) due to unstable thermal conditions (decreasing potential air temperature θ with height)

stations around the lake and meteorological buoys on the lake (Verburg and Hecky 2003). However, our modeling results show that the influence of orography on wind speed spatial variability (e.g. higher wind speed in the center) is higher than the impact of the lake-land breeze system and confirms previous modeling results (Savijärvi 1997).

Wind dynamics is of prime importance for understanding the hydrological cycle of Lake Tanganyika since wind speed and direction drive lake evaporation and precipitation (Verburg and Hecky 2003). More precisely, evaporation increases with rising wind speed (Davarzani et al. 2014). COSMO-CLM^2 modeled latent heat fluxes over Lake Tanganyika are higher in the center and very south of the lake compared to the north (not shown). This correlates with higher wind speed in the center and very south. The diurnal and seasonal cycles of evaporation are controled by the diurnal and seasonal cycles of wind speed: high wind speed over the lake in the early morning (Fig. 7) and during the dry season (Fig. 5) lead to high evaporation rates at those times. With the projected warming over East Africa in the coming decades, evaporation rates are likely to increase (Niang et al. 2014), which could have a profound effect on the hydrological cycle depending on the warming scenario. Furthermore, moisture advection is highly variable from one region to the other due to the presence of high mountains. Therefore, wind profoundly influences precipitation in the vicinity of Lake Tanganyika through lake evaporation and moisture transport. The relationship between wind and hydrological cycle is of crucial importance to understand the future climate of the region.

Another major impact of wind dynamics is on lake hydrodynamics. The classical view of large-scale circulation in Lake Tanganyika is that southeasterly trade winds, which are stronger during the dry season, drive a northward surface current with a southward return flow at the metalimnion depth (Coulter 1991; Plisnier et al. 1999). However, Verburg et al. (2011) conduct a detailed analysis with a three-dimensional numerical lake model in which they find a reversed lake current pattern (southward flow in the upper lake and northward flow in the metalimnion). Therefore, Lake Tanganyika hydrodynamics is still under debate.

The analysis of intraseasonal variability of wind speed shows a 26-day period with secondary cycles around 12, 21 and 36 days (Sect. 3.2). This is in agreement with observations and previous modeling efforts from Naithani et al. (2002, 2003). The latter authors use the Wavelet Transform analysis and find an intraseasonal cycle in the wind speed with a period of the order of 3–4 weeks using observations at Mpulungu (south of the lake) between April 1993 and March 1994. More precisely, the period is 22 days during the dry season and 33 days in the wet season. Using a two-layer reduced-gravity model, they show that the first mode of thermocline oscillation has the same order of magnitude (3–4 weeks). Their study reveals that the free modes of oscillations of the lake are in resonance with wind pulses. This could have a profound impact on lake ecology, e.g. upwelling of nutrients.

The link between wind dynamics and lake hydrodynamics could be further investigated by forcing a three-dimensional hydrodynamic model, such as the one used in Verburg et al. (2011), with output from a high-resolution regional climate model such as presented here.

5 Conclusions

Studying wind speed and direction around Lake Tanganyika is highly important for regional economy (e.g. fishing industry). This study is the first to use a high resolution regional climate model coupled to a lake model to enable an analysis of multi-year (1999–2008) wind dynamics around this lake. Model performance in terms of near-surface wind speed and direction is very good during the dry season (May–August), with modeled wind speed close to QuikSCAT satellite observations. In the wet season, satellite observations overestimate wind speed due to the frequent occurrence of precipitation.

Mean surface wind speed over the lake is higher during the dry season and early morning. In terms of spatial

variability, wind speed is higher over the lake center (and to a lesser extent in the very south) compared to other lake regions, and wind direction in that region is slightly different from other regions. This is due to the presence of troughs in the eastern and western lake shores, which allow the wind to pass through them, leading to wind speed-up and shift in wind direction. This effect is further enhanced by the confluence of two air flows on the upwind side of the lake. The lake center is a region where flow-over conditions persist over a longer period compared to the north and south of the lake. This study also allows to identify a zone of high wind speed at 2 km height associated with the low-level Somali jet.

High wind speed over the lake center is not due to the presence of the lake itself as suggested by the difference in wind speed between a control simulation and a simulation where all lake pixels are replaced by representative land pixels. However, the lake clearly enhances wind speed at certain times of the day (e.g. early morning). Furthermore, a dynamical response induced by the lake is observed, as lake breezes occur during the day (and land breezes at night to a lesser extent).

Finally, this study shows the need for using high resolution modeling combined with satellite observations over a long time period to understand wind dynamics in the vicinity of Lake Tanganyika. This has strong implications for the hydrological cycle, e.g. through evaporation and precipitation, and lake hydrodynamics. These two effects could be further investigated by forcing a three-dimensional hydrodynamic model with output from a high-resolution regional climate model such as presented here.

Acknowledgments We would like to thank Y. Cornet and N. Poncelet for the interesting discussion concerning lake surface water temperature over the African Great Lakes. We also thank I. Gorodetskaya for her input during group discussion. We sincerely thank the editor and two reviewers for their constructive remarks which helped to improve the manuscript. D. Docquier is funded by the Belgian Science Policy Office (BELSPO) through the research project EAGLES. W. Thiery and S. Lhermitte are funded by the Research Foundation Flanders (FWO). The computational resources and services used in this work were provided by the Flemish Supercomputer Center (VSC), funded by the Hercules Foundation and the Flemish Government—department EWI.

References

Akkermans T, Lauwaet D, Demuzere M, Vogel G, Nouvellon Y, Ardö J, Caquet B, De Grandcourt A, Merbold L, Kutsch W, Van Lipzig N (2012) Validation and comparison of two soil-vegetation-atmosphere transfer models for tropical Africa. J Geophys Res 117(G02):013. doi:10.1029/2011JG001802

Akkermans T, Rompaey AV, Lipzig NV (2013) Quantifying successional land cover after clearing of tropical rainforest along forest frontiers in the Congo Basin. Phys Geogr 34(6):417–440. doi:10.1080/02723646.2013.855698

Akkermans T, Thiery W, Van Lipzig NPM (2014) The regional climate impact of a realistic future deforestation scenario in the Congo Basin. J Clim 27(7):2714–2734. doi:10.1175/JCLI-D-13-00361.1

Bentamy A, Grodsky SA, Carton JA, Croiz-Fillon D, Chapron B (2012) Matching ASCAT and QuikSCAT winds. J Geophys Res Oceans. doi:10.1029/2011JC007479

Chakraborty A, Nanjundiah RS, Srinivasan J (2009) Impact of african orography and the indian summer monsoon on the low-level somali jet. Int J Climatol 29(7):983–992. doi:10.1002/joc.1720

Coulter GW (1991) Lake Tanganyika and its life. Oxford University Press, London

Davarzani H, Smits K, Tolene RM, Illangasekare T (2014) Study of the effect of wind speed on evaporation from soil through integrated modeling of the atmospheric boundary layer and shallow subsurface. Water Resour Res 50:661–680. doi:10.1002/2013WR013952

Davin EL, Seneviratne SI (2012) Role of land surface processes and diffuse/direct radiation partitioning in simulating the European climate. Biogeosciences 9(5):1695–1707. doi:10.5194/bg-9-1695-2012

Fore A, Stiles B, Chau A, Williams B, Dunbar R, Rodriguez E (2014) Point-wise wind retrieval and ambiguity removal improvements for the QuikSCAT climatological data set. IEEE Trans Geosci Remote Sens 52(1):51–59. doi:10.1109/TGRS.2012.2235843

Hastings DA, Dunbar PK, Elphingstone GM, Bootz M, Murakami H, Maruyama H, Masaharu H, Holland P, Payne J, Bryant NA, Logan TL, Muller JP, Schreier G, MacDonald JS (1999) The global land one-kilometer base elevation (GLOBE) digital elevation model, version 1.0. http://www.ngdc.noaa.gov/mgg/topo/globe.html

Holton JR (2004) An introduction to dynamic meteorology, 4th edn. Academic Press, London

Kraemer BM, Hook S, Huttula T, Kotilainen P, OReilly CM, Peltonen A, Plisnier PD, Sarvala J, Tamatamah R, Vadeboncoeur Y, Wehrli B, McIntyre PB (2015) Century-long warming trends in the upper water column of Lake Tanganyika. PLoS One 10(7):e0132,490. doi:10.1371/journal.pone.0132490

Mironov DV, Heise E, Kourzeneva E, Ritter B, Schneider N, Terzhevik A (2010) Implementation of the lake parameterisation scheme Flake into the numerical weather prediction model COSMO. Boreal Environ Res 15:218–230

Naithani J, Deleersnijder E, Plisnier PD (2002) Origin of intraseasonal variability in Lake Tanganyika. Geophys Res Lett 29(23):2093. doi:10.1029/2002GL015843

Naithani J, Deleersnijder E, Plisnier P (2003) Analysis of wind-induced thermocline oscillations of Lake Tanganyika. Environ Fluid Mech 3:23–39

Nghiem SV, Leshkevich GA, Stiles BW (2004) Wind fields over the Great Lakes measured by the SeaWinds Scatterometer on the QuikSCAT Satellite. J Great Lakes Res 30(1):148–165. doi:10.1016/S0380-1330(04)70337-8

Niang I, Ruppel O, Abdrabo M, Essel A, Lennard C, Padgham J, Urquhart P (2014) Africa. In: Barros V, Field C, Dokken D, Mastrandrea M, Mach K, Bilir T, Chatterjee M, Ebi K, Estrada Y, Genova R, Girma B, Kissel E, Levy A, MacCracken S, Mastrandrea P, White L (eds) Climate change 2014: impacts, adaptation, and vulnerability. Part B: Regional aspects. Contribution of working group II to the fifth assessment report of the intergovernmental panel on climate change. Cambridge University Press, Cambridge, pp 1199–1265

Nicholson S (1996) A review of climate dynamics and climate variability in Eastern Africa. In: Johnson T, Odada E (eds) The limnology, climatology and paleoclimatology of the East African lakes. Gordon and Breach, Amsterdam, pp 25–56

Plisnier P, Chitamwebwa D, Mwape L, Tshibangu K, Langenberg V, Coenen E (1999) Limnological annual cycle inferred from physical-chemical fluctuations at three stations of Lake Tanganyika. Hydrobiologia 407:45–58

Reinecke PA, Durran DR (2008) Estimating topographic blocking using a Froude number when the static stability is nonuniform. J Atmos Sci 65:1035–1048

Savijärvi H (1997) Diurnal winds around Lake Tanganyika. Q J R Meteorol Soc 123:901–918

Savijärvi H, Järvenoja S (2000) Aspects of the fine-scale climatology over Lake Tanganyika as resolved by a mesoscale model. Meteorol Atmos Phys 73(1–2):77–88

Thiery W, Martynov A, Darchambeau F, Descy JP, Plisnier PD, Sushama L, van Lipzig NPM (2014) Understanding the performance of the FLake model over two African Great Lakes. Geosci Model Dev 7(1):317–337. doi:10.5194/gmd-7-317-2014

Thiery W, Stepanenko VM, Fang X, Jöhnk KD, Li Z, Martynov A, Perroud M, Subin ZM, Darchambeau F, Mironov D (2014b) LakeMIP Kivu: Evaluating the representation of a large, deep tropical lake by a set of 1-dimensional lake models. Tellus A 66(21):390. doi:10.3402/tellusa.v66.21390

Thiery W, Davin E, Panitz HJ, Demuzere M, Lhermitte S, van Lipzig N (2015) The impact of the African Great Lakes on the regional climate. J Clim 28(10):4061–4085. doi:10.1175/JCLI-D-14-00565.1

Tierney J, Mayes M, Meyer N (2010) Late-twentieth-century warming in Lake Tanganyika unprecedented since AD 500. Nat Geosci 3:422–425. doi:10.1038/NGEO865

van Lipzig N, Marshall G, Orr A, King J (2008) The relationship between the southern hemisphere annular mode and Antarctic Peninsula summer temperatures: Analysis of a high-resolution model climatology. J Clim 21(8):1649–1668. doi:10.1175/2007JCLI1695.1

Verburg P, Antenucci JP (2010) Persistent unstable atmospheric boundary layer enhances sensible and latent heat loss in a tropical great lake: Lake Tanganyika. J Geophys Res 115(D11):109. doi:10.1029/2009JD012839

Verburg P, Hecky R (2003) Wind patterns, evaporation, and related physical variables in Lake Tanganyika, East Africa. J Great Lakes Res 29:48–61

Verburg P, Hecky R (2009) The physics of the warming of Lake Tanganyika by climate change. Limnol Oceanogr 54:2418–2430

Verburg P, Antenucci JP, Hecky RE (2011) Differential cooling drives large-scale convective circulation in Lake Tanganyika. Limnol Oceanogr 56(3):910–926. doi:10.4319/lo.2011.56.3.0910

Wallace JM, Hobbs PV (2006) Atmospheric Science. Elsevier, Philadelphia